Journal of Ovonic Research Vol. 5, No. 6, December 2009, p. 175 - 185

EFFECT OF Cu DOPING ON THE STRUCTURAL, OPTICAL AND ELECTRICAL PROPERTIES OF CdS NANOPARTICLES

K. S. Rathore*, Deepika, D. Patidar, N.S. Saxena, K. B. Sharma
Semi-conductor & Polymer Science Laboratory, 5-6, Vigyan Bhawan, Department of Physics, University of Rajasthan, Jaipur- 302004, India

Cu doped CdS nanoparticles of about 2 nm diameter have been synthesized by a wet chemical method. X-ray diffraction (XRD) measurements showed that the nanoparticles have the structure of cubic phase. The broadening of XRD patterns indicate that the prepared samples are nanostructured. Transmission electron microscope (TEM) also confirms that particles are about 2nm. Room temperature photoluminescence (PL) spectrum of undoped sample only exhibited a defect related emission peak. For the doped samples, the Cu related emission peak was observed due to relaxation of carrier from excitonic states of host CdS to T_2 level of Cu. The concentration quenching was observed in our experiments. Electrical measurements made on the above samples show that electrical conductivity has strong dependence on the doping concentration, whereas it has a weak dependence on temperature.

(Received December 5, 2009; accepted December 17, 2009)

Keywords: Doping, Band gap, Electrical conductivity, Photoluminescence

1. Introduction

Semiconductor nanoparticles doped with transition metal ions have attracted wide attention due to their excellent luminescent properties [1-3]. The doping of transition metal ion such as Mn, Cu, Co etc opens up possibilities of forming new class of material and new properties of the material are expected. The transition metal doped nanoparticles show different optical properties corresponding to their host counterparts. These nanoparticles have found tremendous application in optical light emitting diodes [4-7].

In undoped II-VI semiconductors such as CdS , CdTe, CdSe and ZnS, the band gap is engineered by controlling the crystal size, leading to a tunable band edge emission. By doping the nanoparticles with luminescent activators, the excitation can be tuned by quantum size effect while the activator related emission is largely unchanged.

Various effort have been made by the researchers to dope transition metal ions in nanomaterials. P.H. Borse et al [8] have reported the luminescence quenching in ZnS nanoparticles due to Fe and Ni doping. They found that the blue light emission in ZnS nanoparticles could be completely quenched when doped with iron and nickel. M. Marandi et al [9] have studied the thermo-mechanical growth of Mn doped CdS nanoparticles and found that a prolonged reaction time decreases the intensity of Mn luminescence peak to about 35% of the original value.

Doped nanostructured II–VI semiconductors have been used extensively due to their industrial implementation in nanoelectronic devices [10-11]. It would be interesting to study the electrical properties of pellets of transition metal doped nano-particles of semiconductors and the effect on the electrical properties due to increase in temperature for its implementation in the device fabrication.

* Corresponding author. Email: kuldeep_ssr@yahoo.com

In view of this, the present paper reports the structural and optical characterization of the CdS:Cu nanoparticles at room temperature. Besides this, an effort has also been made to study of electrical properties of the CdS:Cu nanoparticles at room temperature as well as elevated temperatures.

2. Experimental details

Nanoparticles of CdS and CdS:Cu have been prepared by chemical precipitation method. All the chemicals were of analytical grade and were used without further purification. Nanoparticles of CdS were prepared at 300 K by dropping simultaneously 50 ml of molar solution of $CdSO_4$ and 50 ml of molar solution of Na_2S into 200 ml of distilled water containing 50 ml of 0.1 M solution of EDTA, which was vigorously stirred using a magnetic stirrer. The high insolubility of CdS formed out of the chemical reaction caused the formation of a number of new nuclei while preventing the growth of already existing ones, thus limiting the particle size.

For the preparation of CdS:Cu nanoparticles, a 50 ml solution of $CuSO_4$ was dropped along with solutions of $CdSO_4$ and Na_2S in the initial stages of preparation. The rest of the process was same as in the case of preparation of pure CdS nanoparticles. The percentage of Cu was varied from 2-8 wt % by adding 2-8 wt% of metal sulphate ($CuSO_4$) to $CdSO_4$. The precipitate was separated from the reaction mixture and was dried at room temperature. After sufficient drying, the precipitate was crushed to fine powder with the help of mortar and pestle. The pure sample has been named as C-1, while the doped samples have been named as CDC-1, CDC-2, CDC-3 and CDC-4 for 2, 4, 6, 8 wt% of Cu respectively.

The wide angle X-ray diffraction pattern of the samples were obtained using Bragg-Brentanno geometry on Panalytical X'pert Pro diffractometer in 2θ range of 15-80^o with CuKα radiation source (λ= 1.5406 Å). The X-ray tube was operated at 45 kV and 40 mA. TEM measurements of the samples were carried out using a Hitachi transmission electron microscope. Samples for the TEM were prepared by making a clear dispersion of nanoparticles in dimethyl formaldehyde and putting a drop of it on a carbon coated copper grid. The EDAX measurements of the synthesized nanoparticles were performed to confirm the copper doping using a FEI Quanta 200F SEM fitted with an EDAX. The optical absorption spectra of the nanoparticles were recorded using ocean optics USB 2000 spectrophotometer in the solution form. The PL emission spectra of all the samples have been recorded at 300 K by using JOBIN YVON (HORIBA) Fluoromax-3 in the powder form. DC electrical conductivity of the pellet was measured by applying 10 V dc across the sample for a short interval and measuring the resistance of the sample using KEITHLEY-6517A electrometer in the V/I mode.

3. Results and discussion

The so-prepared nanoparticles are characterized through XRD, TEM, UV-Vis spectrophotometer, Fluorometer and Electrometer. In the section below, we will discuss these measurements one by one.

3.1 XRD measurements

The nanostructure of the so prepared nanoparticles has been studied at room temperature by using X-ray diffraction pattern. Fig. 1 shows the XRD patterns of all samples of CdS and Cu doped CdS nanoparticles. As expected, the XRD peaks of nanoparticles are considerably broadened due to finite size of these particles. Three diffraction peaks appearing for all the samples at 2θ values of about 26.55, 44.03and 52.08 correspond to the (111) , (220) and (311) planes of cubic phase of CdS. The addition of Cu to CdS nanoparticles does not create any change in the CdS matrix. The XRD data was refined by removing the broadening due to instrumental and non uniform stain present in the lattice.

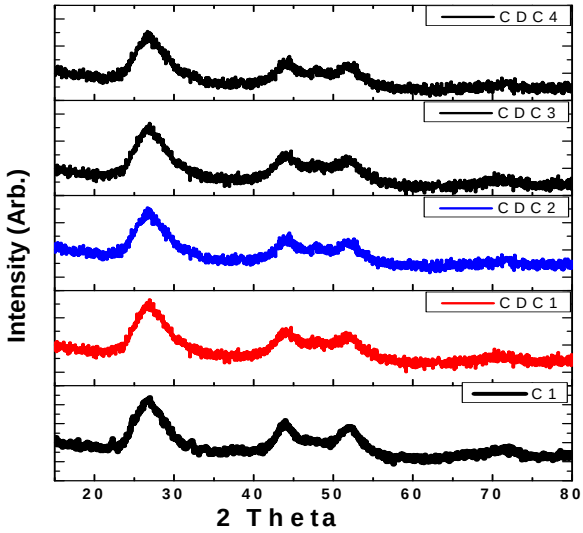

Fig. 1. XRD pattern of all samples

The particle size was calculated using the Scherrer's formula [12]. The Scherrer formula is given by:

$$D = 0.9\ \lambda / \beta \cos\theta \qquad (1)$$

where D is the average particle size perpendicular to the reflecting planes, λ is the X-ray wavelength, β is the full width at half maximum (FWHM), and θ is the diffraction angle. The average particle size of C 1,CDC 1, CDC 2, CDC 3and CDC 4 were found to be 1.6 nm 1.6 nm , 1.5 nm,.1.42 nm and 1.3 nm respectively.

3.2 TEM measurements

Fig. 2A shows the TEM image of sample C 1 (Pure CdS) and sample CDC 1 as a representative image of Cu Doped CdS. It shows abundance of spherical particles, whose size distribution is given by the histogram as shown in Fig. 2b. The size of the particle of CDC 1 estimated through TEM is found to be ~ 2 nm. The particle sizes of CDC 2, CDC 3 and CDC 4 as obtained from TEM measurements were found to be 1.9 nm, 1.8 nm and 1.7 nm respectively.

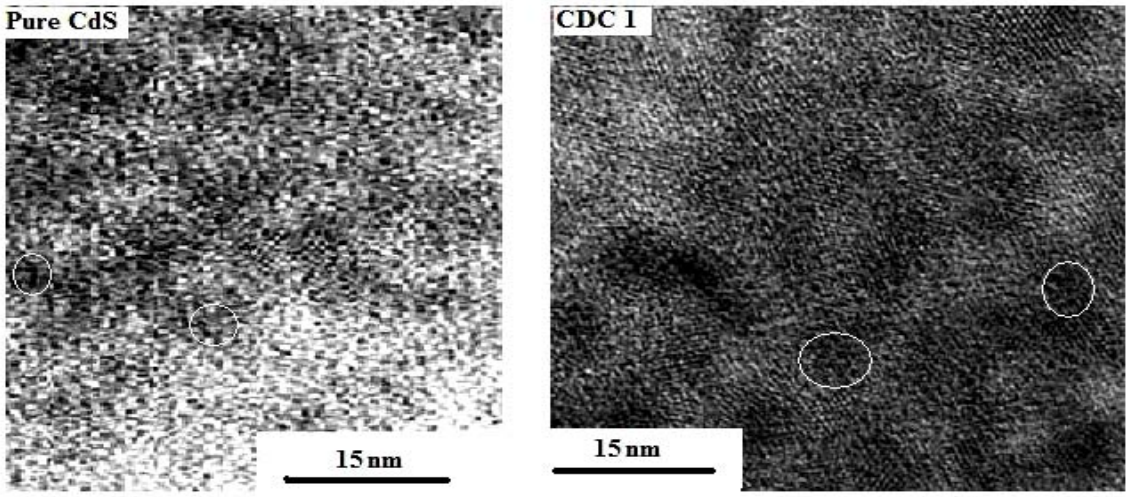

Fig.2a. TEM image of Pure and Cu doped (2 wt%) CdS samples

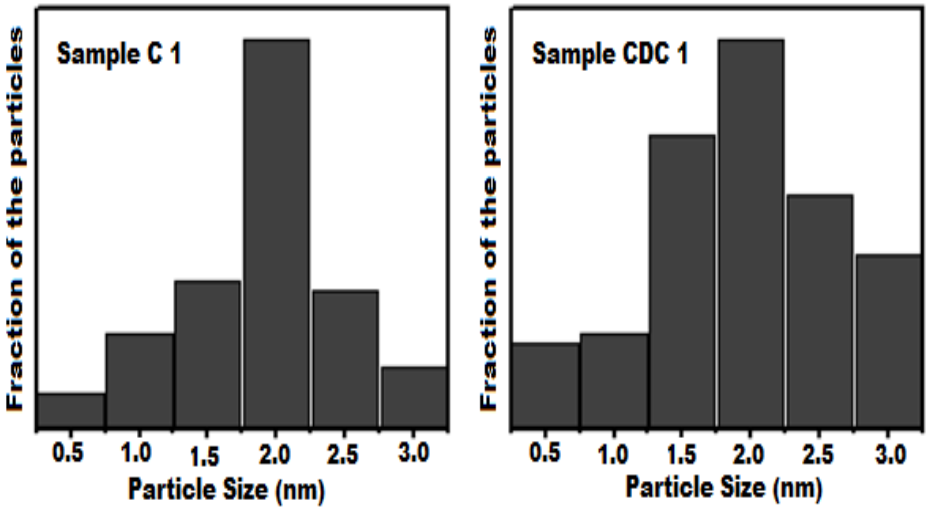

Fig. 2b. Histogram of Pure and Cu doped (2 wt%) CdS samples

The particle sizes obtained from TEM are slightly larger than that estimated through XRD results. This type of mismatching in particle sizes estimated from TEM and XRD has also been reported earlier [13]. The slight discrepancy is due to the intrinsic defects like twining and dislocations present in the lattice of these samples. Table 1 lists the values of particle size of all the samples using XRD and TEM.

Table 1. Values of particle sizes of all the sample through XRD and TEM

Sample Code	Particle Size through TEM (nm)	Particle Size through XRD (nm)
C 1	2	1.6
CDC 1	2.1	1.6
CDC 2	1.9	1.5
CDC 3	1.8	1.4
CDC 4	1.7	1.3

3.3 Energy Dispersive Analysis of X-rays (EDAX)

EDAX of powder sample of CDC-1 (Fig. 3) shows cadmium, sulphur and copper to be in a stoichiometric atomic ratio. The EDAX of all the samples depict the successful doping of copper in the lattice of CdS nanoparticle.

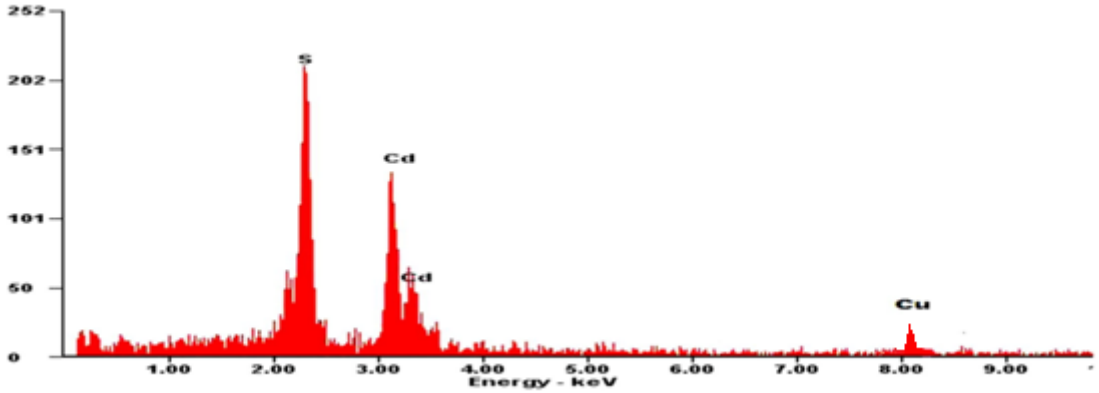

Fig. 3. EDAX of Cu doped (2 wt %) CdS nanoparticle

3.4 Optical measurements

The absorbance versus wavelength traces for all samples have been recorded in the range 300-700 nm as shown in Fig. 4. The absorption, which corresponds to electron excitation from the valence band to conduction band, can be used to determine the nature and value of the optical band gap. The relation between the absorption coefficients (α) and the incident photon energy ($h\nu$) can be written as [14]:

$$(\alpha h\nu) = A\,(h\nu - E_g)^n \qquad (2)$$

where A is a constant and E_g is the band gap of the material and exponent n depends on the type of transition. For direct allowed n = 1 /2, indirect allowed transition, n = 2, and for direct forbidden, n =3/ 2.

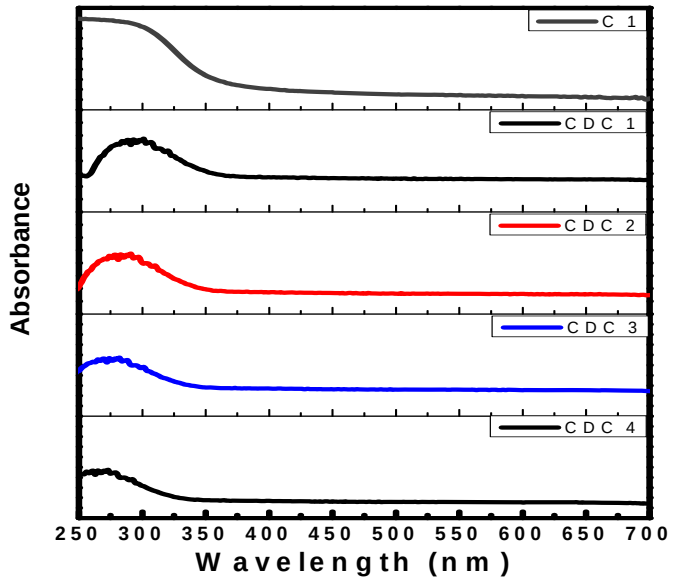

Fig 4. The absorbance versus wavelength plots for all the samples

To measure the energy band gap from the absorption spectra a graph $(\alpha h\nu)^2$ versus $h\nu$ is plotted (Fig. 5). The extrapolation of the straight line to $(\alpha h\nu)^2 = 0$ axis gives the value of the energy band gap. The direct allowed band gap values of C-1, CDC-1, CDC-2, CDC-3, and CDC-4 have been found to be 3.7 eV, 3.83 eV, 3.88 eV, 3.93 eV and 3.98 eV respectively. The absorption edge shifts towards the lower value of wavelength (higher energy) with a increase in concentration of Cu . It is clear that band gap increase with doping concentration slightly. The trend of observed band gap variation after doping in present study is similar to that reported earlier [15-16]. In our system, it is postulated that the number and rate of nucleation is increased with Cu^{2+} doping concentration because of lesser solubility of CuS, which produces relatively small particle leading to quantum confinement effect.

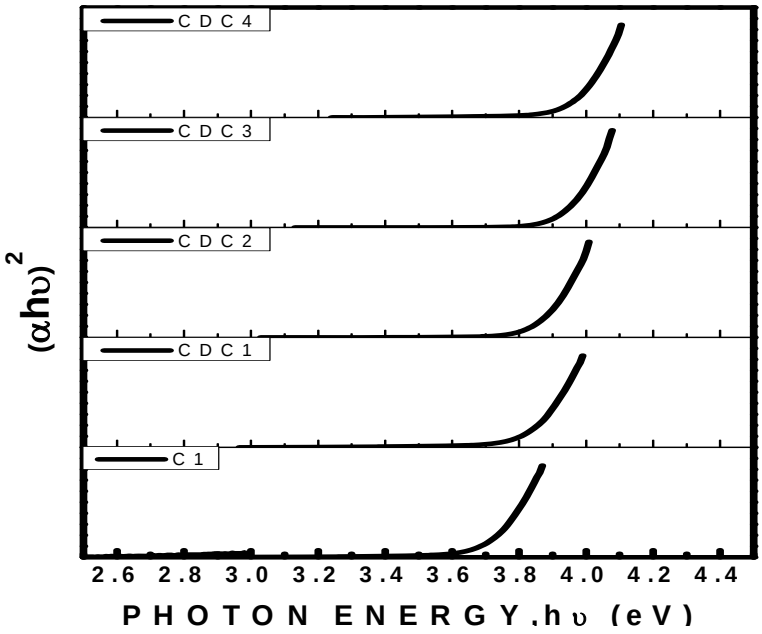

Fig. 5. Plots of $(\alpha h\nu)^2$ versus $h\nu$ for all the samples

3.5 Photoluminescence

Photoluminescence emission spectra (at 300 K) of all the samples excited at 300 nm has been shown in Fig. 6. Sample C 1 shows a peak centered at 545 nm. The broad emission centered at 545 nm is attributed to carrier recombination at surface states. It could be due to either sulphur vacancies or cadmium vacancies depending on the availability of the cations or anions [17]. This broad emission centered at 545 nm is due to cadmium vacancies at the surface of sample C 1.

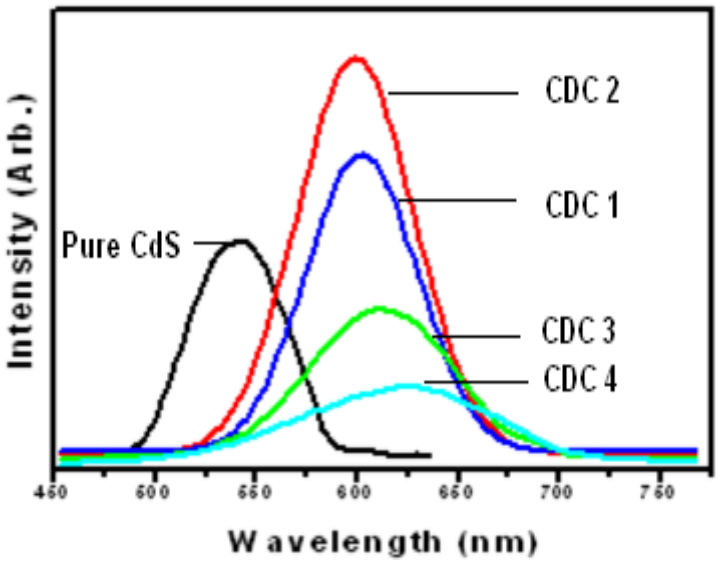

Fig. 6. Emission spectra of all the samples.

The surface states due to Cd vacancies can act as hole trap states. Hence, the broad emission at ~ 545 nm is attributed to relaxation of carriers from the excitonic to the surface trap

states. This can be assumed to be located at ~ 2.2 eV below the conduction band as shown in Fig. 7. This implies that the trap state due to Cd^{+2} vacancies are located at ~ 1.5 eV above the valence band also shown in Fig. 7. This is in reasonable agreement with earlier reports that states due to Cd vacancies in CdS lie in the range of 0.25 eV -1.5 eV above the valence band [18-19]. The broad surface state emission indicate that the surface state also have a finite distribution due to the size variation of nanoparticles.

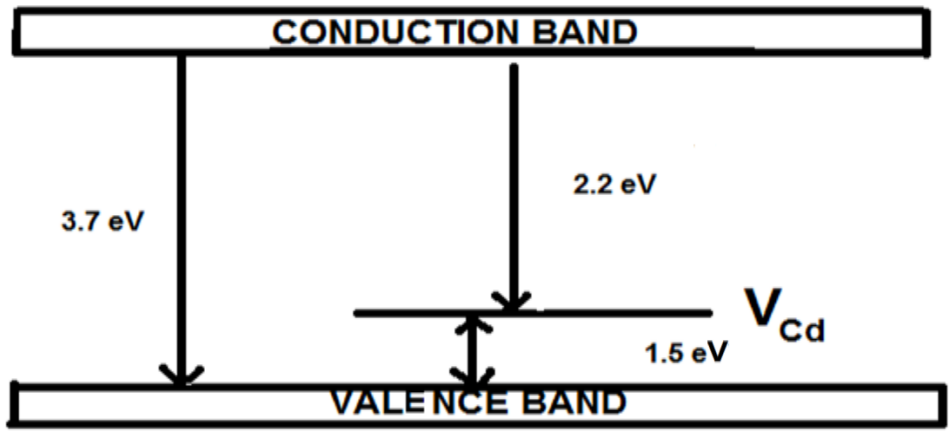

Fig. 7. Schematic energy levels of CdS nanoparticles.

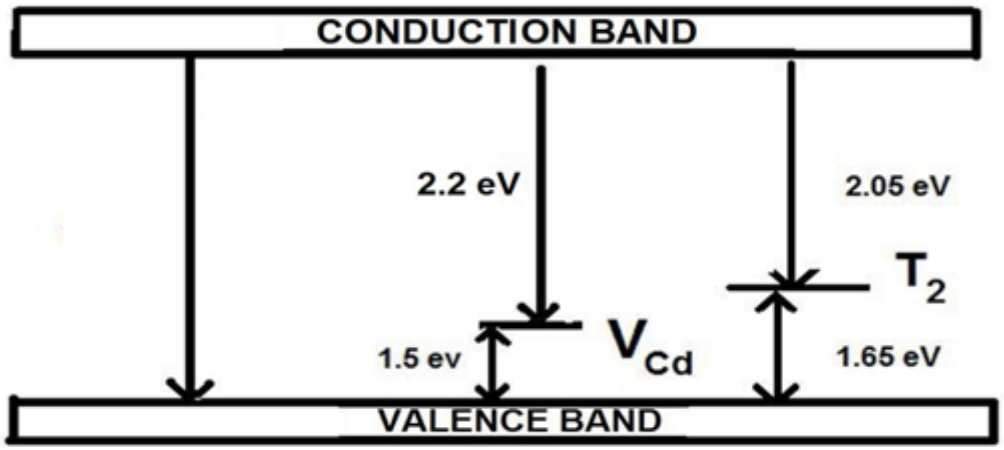

Fig. 8. Schematic energy levels of Cu doped CdS nanoparticles

The PL emission spectra of Cu doped CdS samples show that Cu related orange-red emission is centered at ~ 601 nm. The Cu related emission may be attributed to the relaxation of carriers from excitonic states of host CdS to T_2 level of Cu, which in such a case lie at 1.65 eV above the ground state as shown in Fig 8. This accepter level has been assigned to the T_2 level in tetrahedrally coordinated Cu in CdS. Further, on the basis of density functional electronic structure calculation, it has also been reported the substitutional Cu in CdS, formed under sulphur rich condition generate an acceptor level with low energy [20]. It may also be noted that the ionic radius of four coordinated (square-planer) Cu^{++} is 0.57 Ă, which is smaller than the value of 0.78 Ă for four co-ordinated Cd^{++} [21]. On the basis of above statement , it is reasonable to infer the formation of tetrahedrally coordinated substitutional Cu in CdS and attribute the strong orange-red luminescence to relaxation from excitonic level of CdS to T_2 level .

With the increase of Cu^{2+} concentration, the intensity of the orange red emission significantly increases while its peak position does not shift upto 4 wt% of copper . Beyond 4 wt% of Cu doping, quenching phenomenon occurred in the system. Concentration quenching has been mainly attributed to the migration of excitation energy between Cu^{2+} ion pair in the case of doping concentration beyond 4 wt%. Thus the existence of Cu^{2+} pairs is important for occurrence of the concentration quenching effect. During the concentration quenching process, the excitation energy is transferred from one Cu^{2+} ion by nonradiative transition and via a number of transfer steps finally to quenching site (eg. defect site). Such a decrease in intensity with increasing copper loading was also reported by Wang et al. [22]

The PL spectra show red shift on doping. The red shift of emission spectra peak may be due to the indirect recombination of free electrons moving from trap level formed by Cu atoms to the holes in valence band . These trap levels are in energy gap and shift towards the valence band on doping [23]. In other words the localized energy level of exciton states of Cu^{2+} is different from that of Cd^{2+}, which leads to a shift of PL peak.

3.6 Electrical Studies

The conductivity of all the sample have been determined by I-V measurement using the electrometer at room temperature. The temperature dependent conductivity for samples C 1, CDC 1 and CDC 2 have also been determined by I-V measurement over the temperature range from room to 373 K. Fig. 9 shows the typical room temperature I-V characteristics of all the samples.

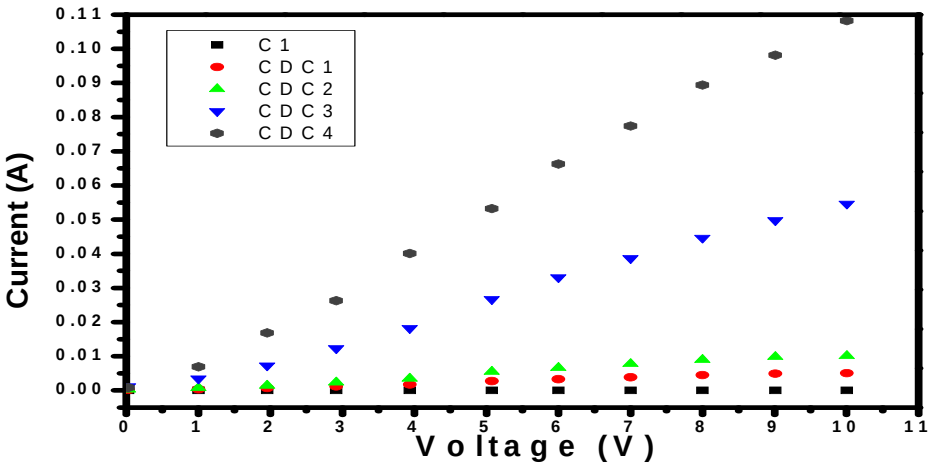

Fig. 9. I-V characteristics of all the samples at the room temperature.

Fig. 9 shows the almost linear behavior of current with applied voltage. DC Electrical conductivity was calculated from the relation.

$$\sigma_{dc} = 1/\rho \qquad \text{(where } \rho = RA/L\text{)}$$
$$= L/RA$$

where R is the resistance of the sample (slope of the linear region of I-V curve gives us the value of the resistance for that particular sample), L is the thickness of the particular sample (which is 0.155 cm for all the sample), A is the cross sectional area of the sample (which is 1.1304 cm^2 for all the samples, because the radius of pellet for each sample is 0.6 cm) and ρ is the resistivity of the sample under test.

Table 2 shows the values of conductivities for all five samples at room temperature measurement.

Table 2. Conductivities for all five samples at room temperature.

Sample Code	Cu in wt% in CdS	Conductivity (S /cm)
C1	0	1.51×10^{-7}
CDC 1	2	7.5×10^{-5}
CDC 2	4	1.52×10^{-4}
CDC 3	6	7.58×10^{-4}
CDC 4	8	1.52×10^{-3}

From Table 2, it is evident that sample CDC 4 gives maximum conductivity while C 1 has the lowest conductivity at room temperature among all the samples. It is found that on increasing the Cu^{2+} concentrations in CdS nanoparticles current increases, which may be due to incorporating the copper impurity for Cd sites and availability of free electrons. These results are in good agreement with previously reported results that doping was found to change the electrical conductivity [24-25]. Electrical conduction is assumed to take place between the CdCuS nanoparticles. However, a wide range of different currents are recorded for different concentration of the Cu^{2+} ions in the samples. In view of above results (Table 2), pure CdS (C1), lowest Cu doped CdS sample (CDC 1) and the highest Cu doped CdS sample (CDC 4) have been chosen to see the effect of temperature on their conductivity with doping concentration.

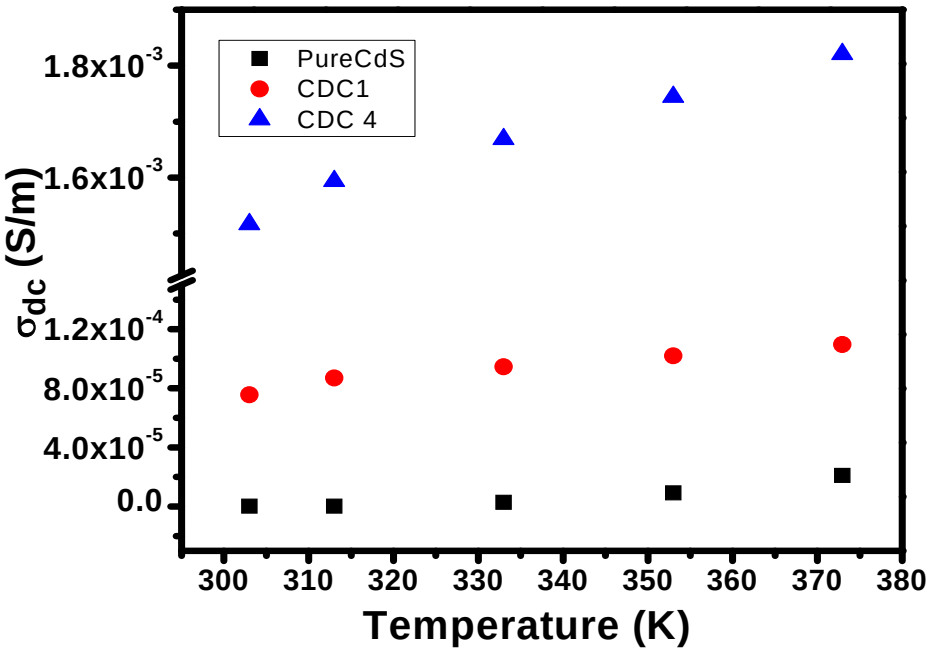

Fig. 10. Temperature versus conductivity curve for samples C1, CDC 1 and CDC 4.

Temperature dependence DC electrical conductivity of sample C1, CDC 1 and CDC 4 have been shown in Fig. 10. From Fig. 10, it is observed conductivity increases almost linearly with temperature for these three samples. This increase in conductivity with increase of temperature is attributed to improvement of charge density. Due to temperature effect, the inter-grain boundary area decreases i.e. there is a decrease in the scattering of the electron. Consequently, the carrier concentration and mobility in the inter-grain domains also increase. This inturn increases the conductivity.

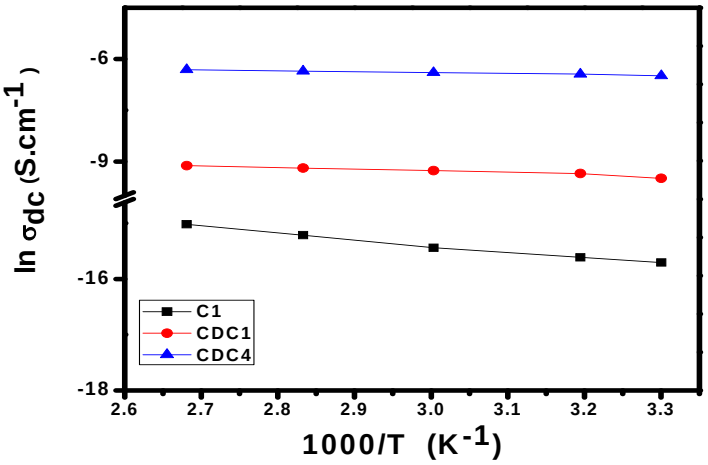

Fig. 11. Variation of ln σ_{dc} of CdS nanoparticle with 1000/T.

The temperature dependence of electrical conductivity (σ_{dc}) of above mentioned two samples follows the Arrhenius model and is given by

$$\sigma = \sigma_o \exp (\quad E_a / kT)$$

where σ_o is the pre-exponential factor, E_a is the activation energy of the electrical conduction, k

is the Boltzmann constant and T is the absolute temperature. Fig. 11 shows the graph between ln(σ) versus 1000/T. From this graph, the activation energy has been determined for these three samples, listed in table 3.

Table 3. Values of conductivity at room temperature and activation energy for C 1, CDC 2 and CDC 3 samples.

Sample Code	Conductivity at room temp (S/cm)	Activation Energy (eV)
C 1	1.51×10^{-7}	1.10
CDC 1	7.5×10^{-5}	0.55
CDC 4	1.52×10^{-3}	0.28

From table 3, it is observed that the value of activation energy of electrical conduction is lowest for sample CDC 4, which confirms the higher conductivity of sample CDC 4 among all samples.

4. Conclusions

A systematic study of structural, optical and electrical properties of CDS and CdS:Cu nanoparticles leads to the following conclusions:

1. The structural characterizations done through XRD and TEM reveal that the prepared samples are nanocrysatlline in nature and their particle size shows a decreasing trend with the increase in doping concentration of Cu in CdS nanoparticles.
2. The band gap of all the samples increases with the increase in doping concentration of Cu in CdS nanoparticles. This increase is the outcome of quantum confinement effect originated from smaller size of nanoparticles produced at higher concentration of Cu doping.

3. The PL emission spectra of Cu doped CdS samples show that Cu related orange-red emission is centered at ~ 601 nm. The Cu related emission may be attributed to the relaxation of carriers from excitonic states of host CdS to T_2 level of Cu.

4. At room temperature as well as at elevated temperature, the electrical conductivity of the samples increases with the increase in doping concentration of Cu in CdS nanoparticles. This is due to the increased carrier density of free electrons.

References

[1] J. Nanda, S . Sapra, D. D. Sarma, Chem. Mater. **12**, 1018 (2000).
[2] R. N. Bhargava, D. Gallagher, X. Hong, A. Nurmikko, Phys. Rev. Lett. **72**, 416 (1994).
[3] M. A. Olshavsky, H. R. Allcock, Chem. Mater. **9**, 1367 (1997).
[4] L. S . Dong, X. F . FU, M. W. Wang, C. H. Liu, J. Lumin. **87–89**, 538 (2000).
[5] N. Francois, B. Ginzberg, S . A. Bilmes, J. Sol- Gel Scitechn. **13**, 341 (1998).
[6] R. Premachandran, S . Banerjee, V. T. John, G. L. Mcpherson, J . A. Akkara, D. L. Kaplan, Chem. Mater. **9**, 1342 (1997).
[7] M. Y. Gao, X. Zhang, B. Yang, F . Li, J . C. Shen, Thin Solid Films. **284-285**, 242 (1996).
[8] P.H. Borse, N.Deshmukh, R.F. Shinde, S.K. Date, S.K. Kulkarni, J. Mater.Sci. **34**, 6087 **(**1999).
[9] M. Marandi, N. Taghavinia, Z. Sedaghat, A. Irajizad , S.M. Madhvi, Nanotechnology **19**, 225705 (2008).
[10] S. Sampra, D.D. Sarma, Phys. Rev. B **69**, 125304 (2004).
[11] N. Karar, F. Sing, B.R. Mehta, J. Appl. Phys. **95**, 656 (2004).
[12] T .P. Sharma , D. Patidar, N .S. Saxena, K .Sharma, Ind. J. Pure & Appl. Phys. **44**, 125 (2005).
[13] J. Nanda, S. Sapra, D.D. Sarma, Chem. Mater.**12**, 1018 (2000).
[14] D. Patidar, K.S. Rathore, N.S. Saxena, K.B. Sharma, T.P. Sharma, J. Nano Res. **3**, 97 (2008).
[15] K. Jayanthi, S. Chawala, H. Chander, D. Haranath, Cryst. Res. Technol. **42**, 976 (2007).
[16] W. Sang, Y. Quian, J. Min, D. Li, L. Wang, L. Yinfeng, Solid State Comm. **121**, 475 (2002).
[17] P. Mandal, S.S. Talwar, S.S. Major, R.S. Srinivasa, J. Chem. Phys **128**, 114703 (2008).
[18] R.H. Bube, Photoconductivity of Solids, Wiely, New York (1960).
[19] I.J. Ferrer, P. Salvador, J. Appl. Phys.**66**, 2568(1989).
[20] K. Nishidate, T. Sato, Y. Matsukena, M. Baba, M. Hasegawand, T. Sasaki, Phys. Rev. B **74**, 35210 (2006).
[21] D.R. Linde, Handbook of Chemistry and Physics, 79th ed. CRC, Washingaton, DC (1998).
[22] M. Wang, L.Sun, X.Fu, C. Liao, C.Yan, Solid State comm. **115**, 493 (2000).
[23] P.Roy, S.K. Srivastava, J. Phys. D. Appl. Phys. **39**, 4771 (2006).
[24] M. Ikeda, K.Itoh, H.Sato, J.Phys. Soc. Jpn. **25**, 455 (1968).
[25] B.Tripathi, F. Singh, D.K. Avasthi, A.K. Bhati, D.Das, Y.K. Vijay, J. Alloys Comp. **454**, 97(2008).